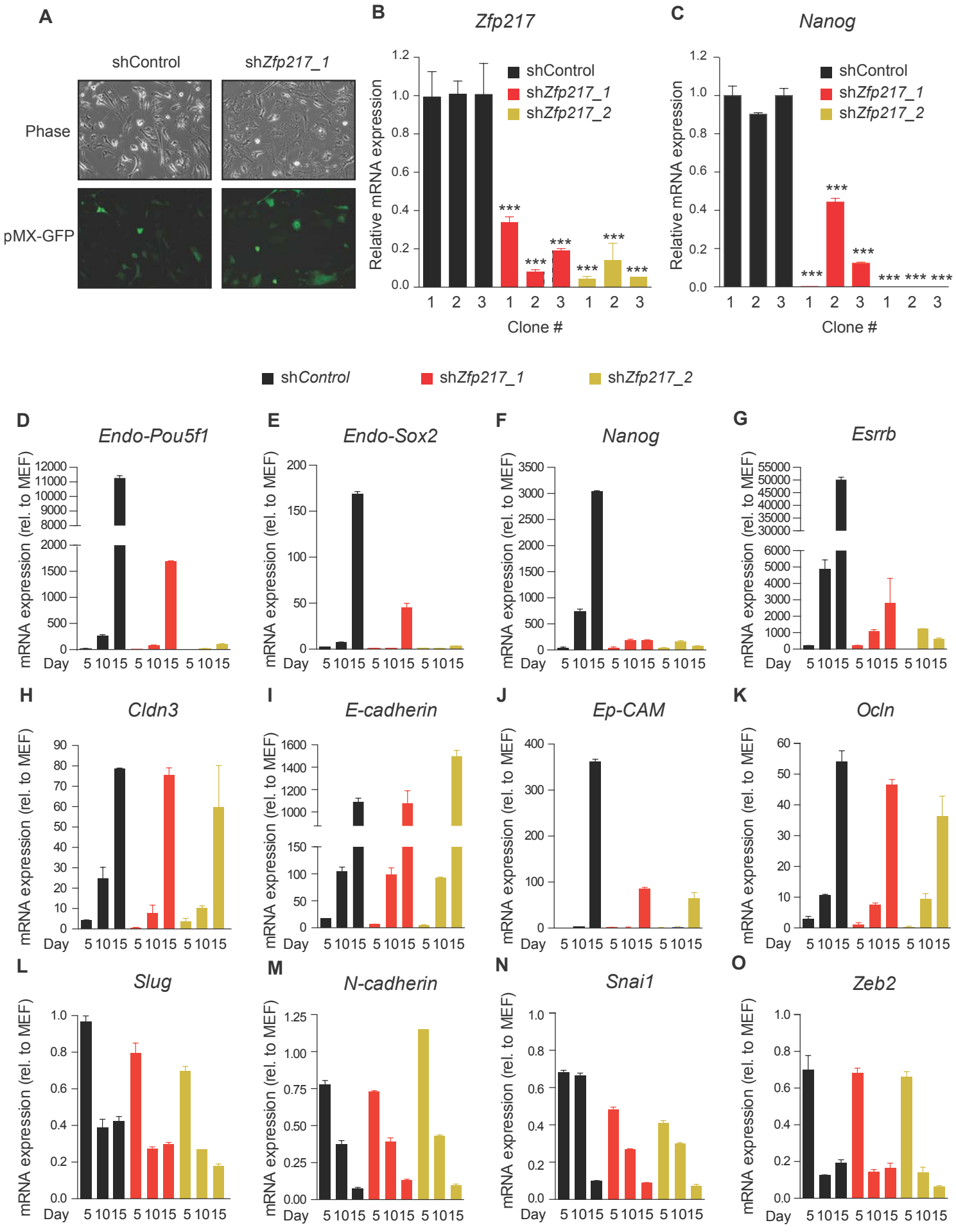
A
shControl
shZfp217_1
Phase
pMX-GFP
B
Zfp217
Relative mRNA expression
shControl
shZfp217_1
shZfp217_2
Clone #
C
Nanog
Relative mRNA expression
shControl
shZfp217_1
shZfp217_2
Clone #
shControl
shZfp217_1
shZfp217_2
D
Endo-Pou5f1
E
Endo-Sox2
F
Nanog
G
Esrrb
H
Cldn3
I
E-cadherin
J
Ep-CAM
K
Ocln
L
Slug
M
N-cadherin
N
Snai1
O
Zeb2
mRNA expression (rel. to MEF)
Day

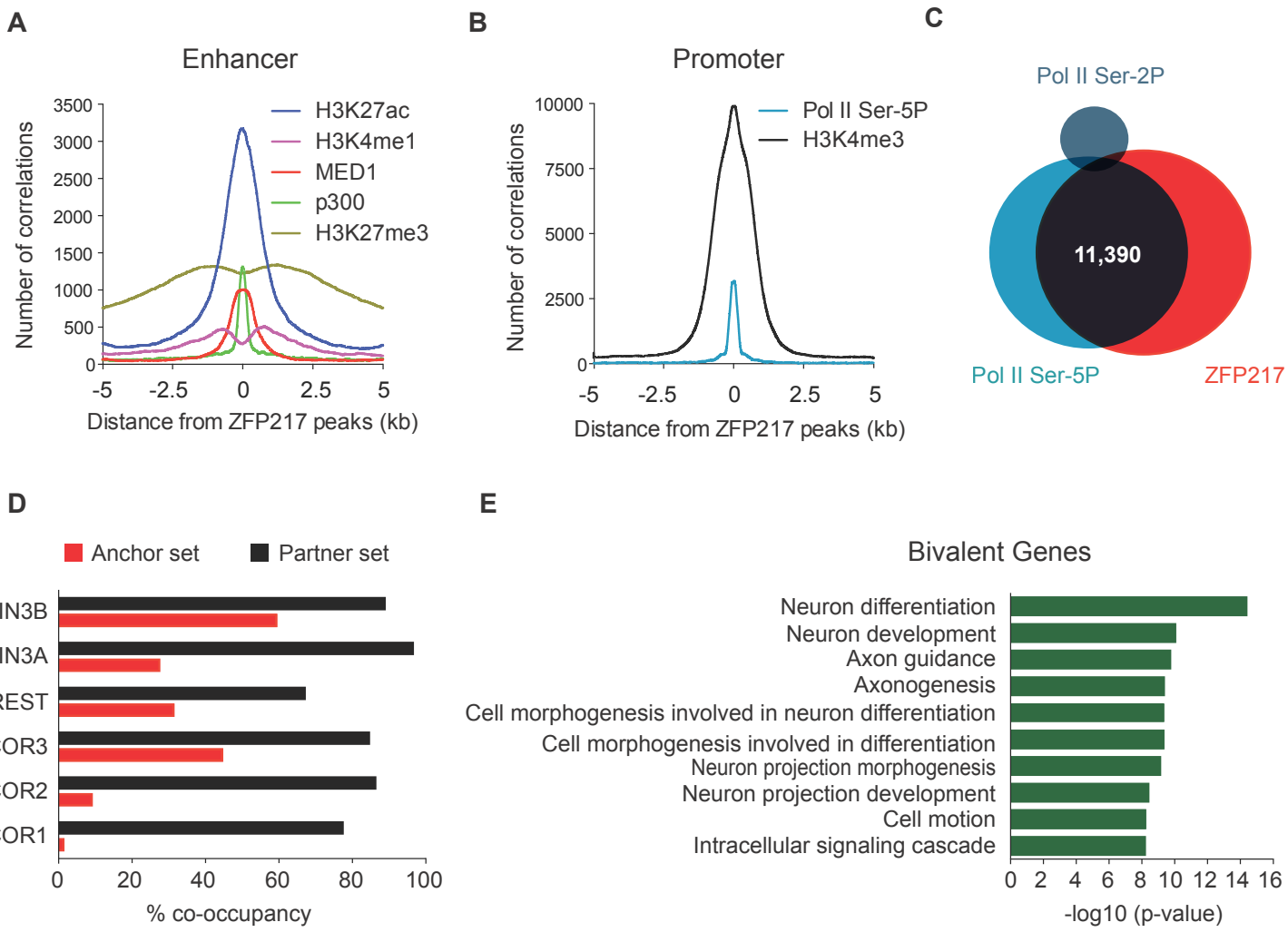
A
Enhancer
Number of correlations
3500
3000
2500
2000
1500
1000
500
0
H3K27ac
H3K4me1
MED1
p300
H3K27me3
-5
-2.5
0
2.5
5
Distance from ZFP217 peaks (kb)
B
Promoter
Number of correlations
10000
7500
5000
2500
0
Pol II Ser-5P
H3K4me3
-5
-2.5
0
2.5
5
Distance from ZFP217 peaks (kb)
C
Pol II Ser-2P
11,390
Pol II Ser-5P
ZFP217
D
Anchor set
Partner set
SIN3B
SIN3A
REST
RCOR3
RCOR2
RCOR1
0
20
40
60
80
100
% co-occupancy
E
Bivalent Genes
Neuron differentiation
Neuron development
Axon guidance
Axonogenesis
Cell morphogenesis involved in neuron differentiation
Cell morphogenesis involved in differentiation
Neuron projection morphogenesis
Neuron projection development
Cell motion
Intracellular signaling cascade
0
2
4
6
8
10
12
14
16
-log10 (p-value)

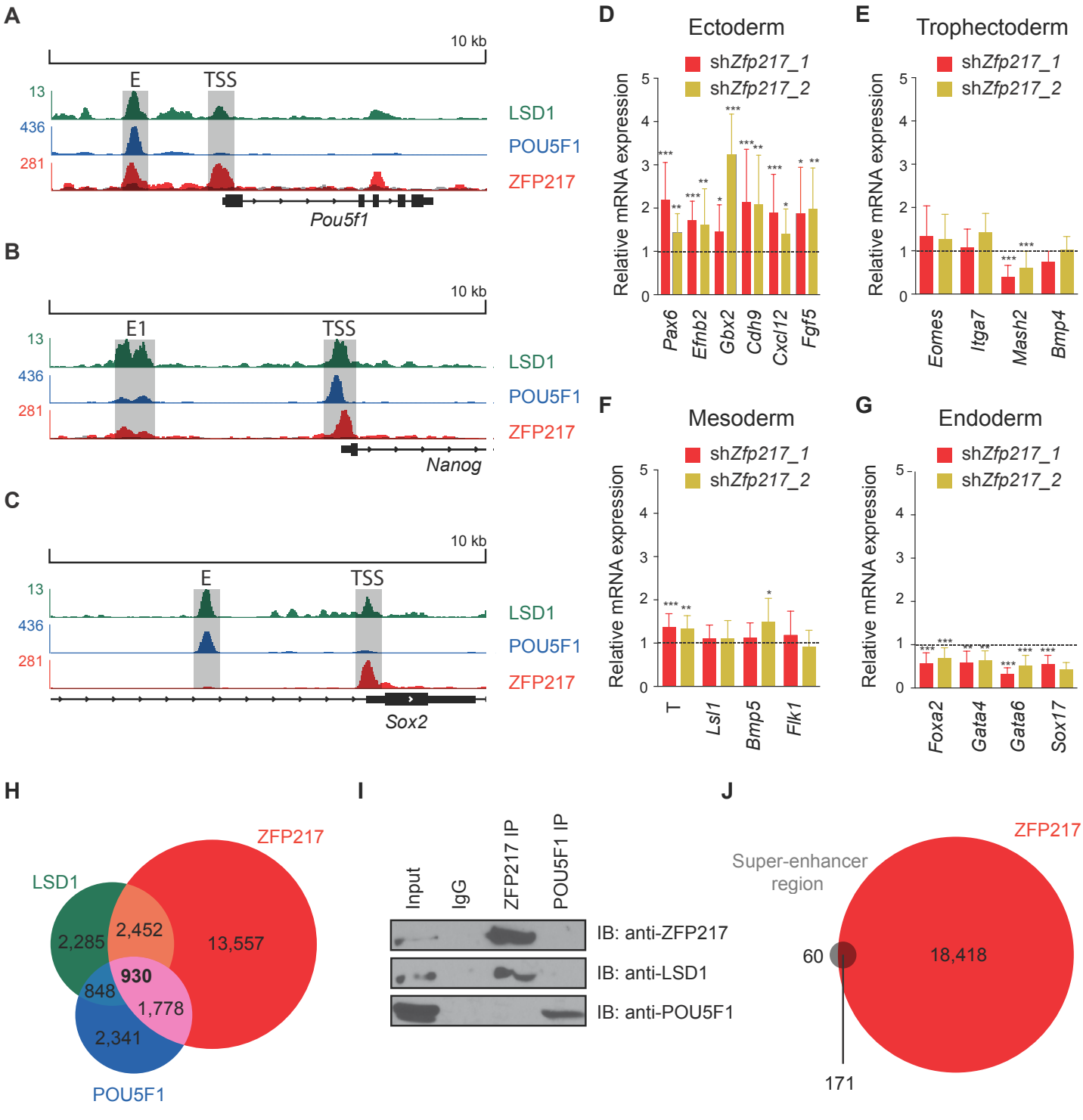
A
10 kb
E
TSS
13
436
281
LSD1
POU5F1
ZFP217
Pou5f1
B
10 kb
E1
TSS
13
436
281
LSD1
POU5F1
ZFP217
Nanog
C
10 kb
E
TSS
13
436
281
LSD1
POU5F1
ZFP217
Sox2
D
Ectoderm
shZfp217_1
shZfp217_2
Relative mRNA expression
Pax6
Efnb2
Gbx2
Cdh9
Cxcl12
Fgf5
E
Trophectoderm
shZfp217_1
shZfp217_2
Relative mRNA expression
Eomes
Itga7
Mash2
Bmp4
F
Mesoderm
shZfp217_1
shZfp217_2
Relative mRNA expression
T
Lsl1
Bmp5
Flk1
G
Endoderm
shZfp217_1
shZfp217_2
Relative mRNA expression
Foxa2
Gata4
Gata6
Sox17
H
ZFP217
LSD1
POU5F1
2,285
2,452
13,557
930
848
1,778
2,341
I
Input
IgG
ZFP217 IP
POU5F1 IP
IB: anti-ZFP217
IB: anti-LSD1
IB: anti-POU5F1
J
ZFP217
Super-enhancer region
60
18,418
171

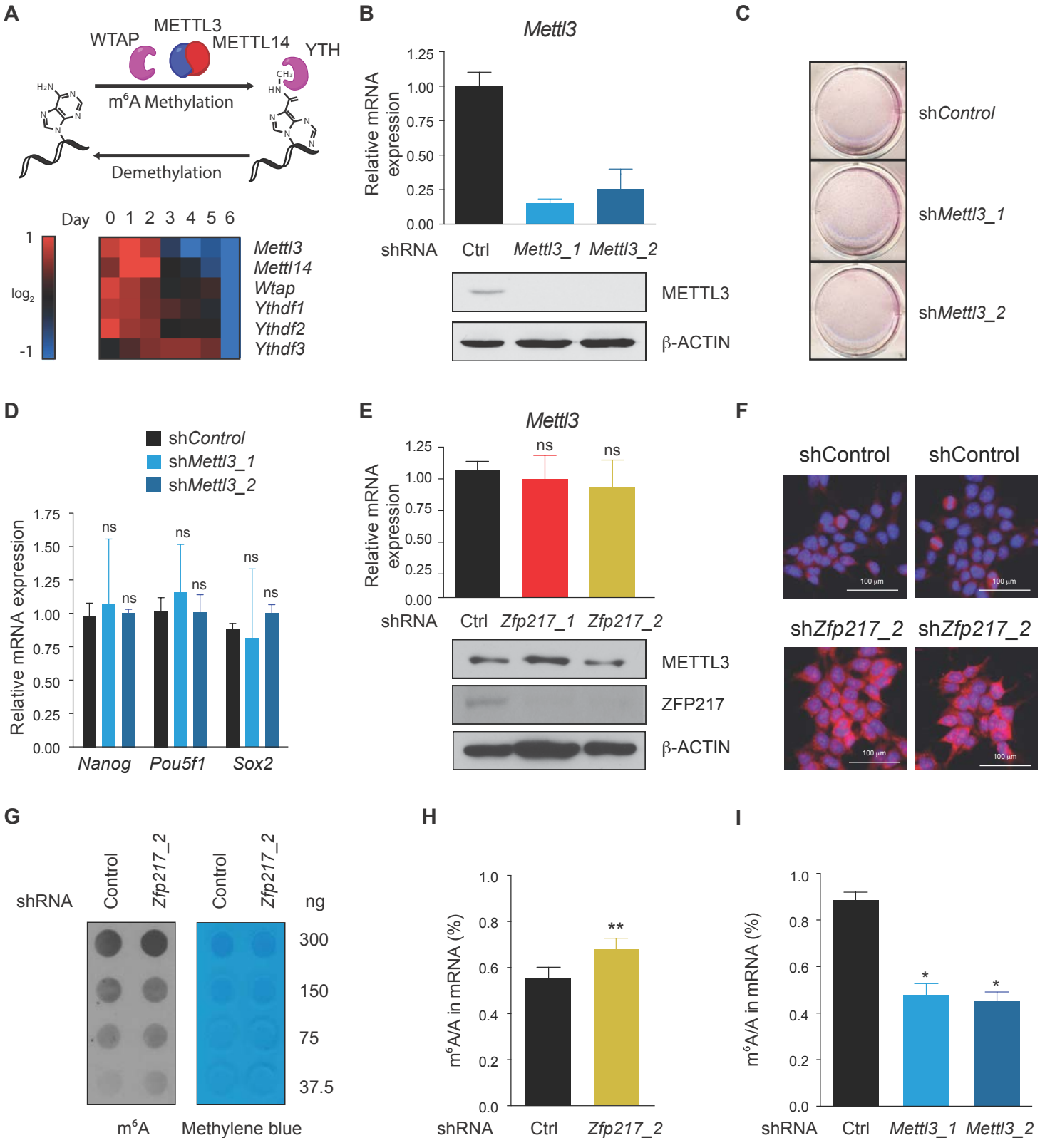
A
METTL3
WTAP
METTL14
YTH
m6A Methylation
Demethylation
Day 0 1 2 3 4 5 6
log2
1
-1
Mettl3
Mettl14
Wtap
Ythdf1
Ythdf2
Ythdf3
B
Mettl3
Relative mRNA expression
1.25
1.00
0.75
0.50
0.25
0.00
shRNA Ctrl Mettl3_1 Mettl3_2
METTL3
β-ACTIN
C
shControl
shMettl3_1
shMettl3_2
D
shControl
shMettl3_1
shMettl3_2
Relative mRNA expression
1.75
1.50
1.25
1.00
0.75
0.50
0.25
0.00
ns
Nanog
Pou5f1
Sox2
E
Mettl3
Relative mRNA expression
ns
shRNA Ctrl Zfp217_1 Zfp217_2
METTL3
ZFP217
β-ACTIN
F
shControl
shControl
shZfp217_2
shZfp217_2
100 μm
G
shRNA
Control
Zfp217_2
Control
Zfp217_2
ng
300
150
75
37.5
m6A
Methylene blue
H
m6A/A in mRNA (%)
1.0
0.8
0.6
0.4
0.2
0.0
**
shRNA Ctrl Zfp217_2
I
m6A/A in mRNA (%)
*
*
shRNA Ctrl Mettl3_1 Mettl3_2

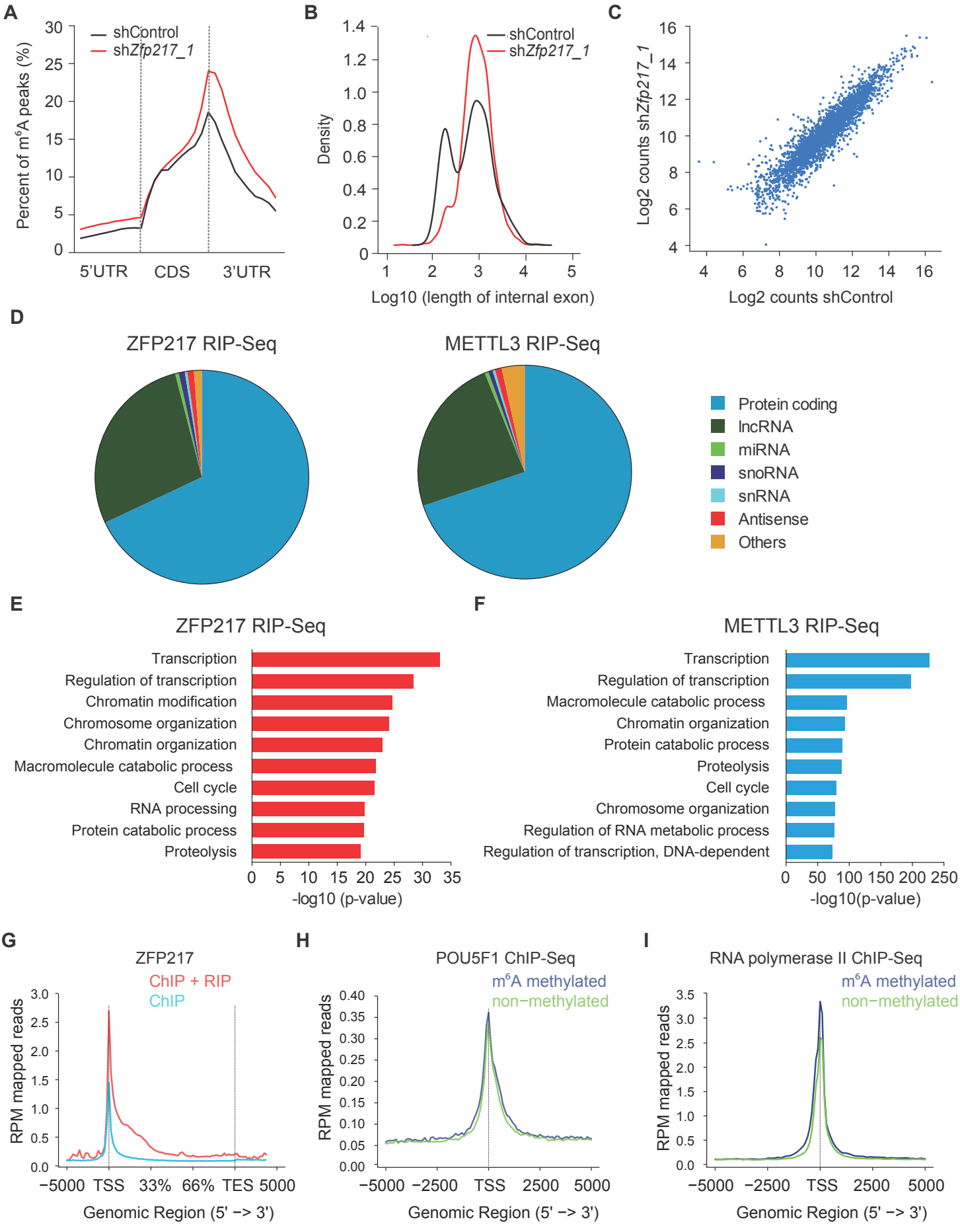
A
Percent of m6A peaks (%)
shControl
shZfp217_1
5'UTR
CDS
3'UTR
B
Density
Log10 (length of internal exon)
C
Log2 counts shZfp217_1
Log2 counts shControl
D
ZFP217 RIP-Seq
METTL3 RIP-Seq
Protein coding
lncRNA
miRNA
snoRNA
snRNA
Antisense
Others
E
ZFP217 RIP-Seq
Transcription
Regulation of transcription
Chromatin modification
Chromosome organization
Chromatin organization
Macromolecule catabolic process
Cell cycle
RNA processing
Protein catabolic process
Proteolysis
-log10 (p-value)
F
METTL3 RIP-Seq
Transcription
Regulation of transcription
Macromolecule catabolic process
Chromatin organization
Protein catabolic process
Proteolysis
Cell cycle
Chromosome organization
Regulation of RNA metabolic process
Regulation of transcription, DNA-dependent
-log10(p-value)
G
ZFP217
ChIP + RIP
ChIP
RPM mapped reads
−5000 TSS 33% 66% TES 5000
Genomic Region (5' -> 3')
H
POU5F1 ChIP-Seq
m6A methylated
non−methylated
RPM mapped reads
−5000 −2500 TSS 2500 5000
Genomic Region (5' -> 3')
I
RNA polymerase II ChIP-Seq
m6A methylated
non−methylated
RPM mapped reads
−5000 −2500 TSS 2500 5000
Genomic Region (5' -> 3')

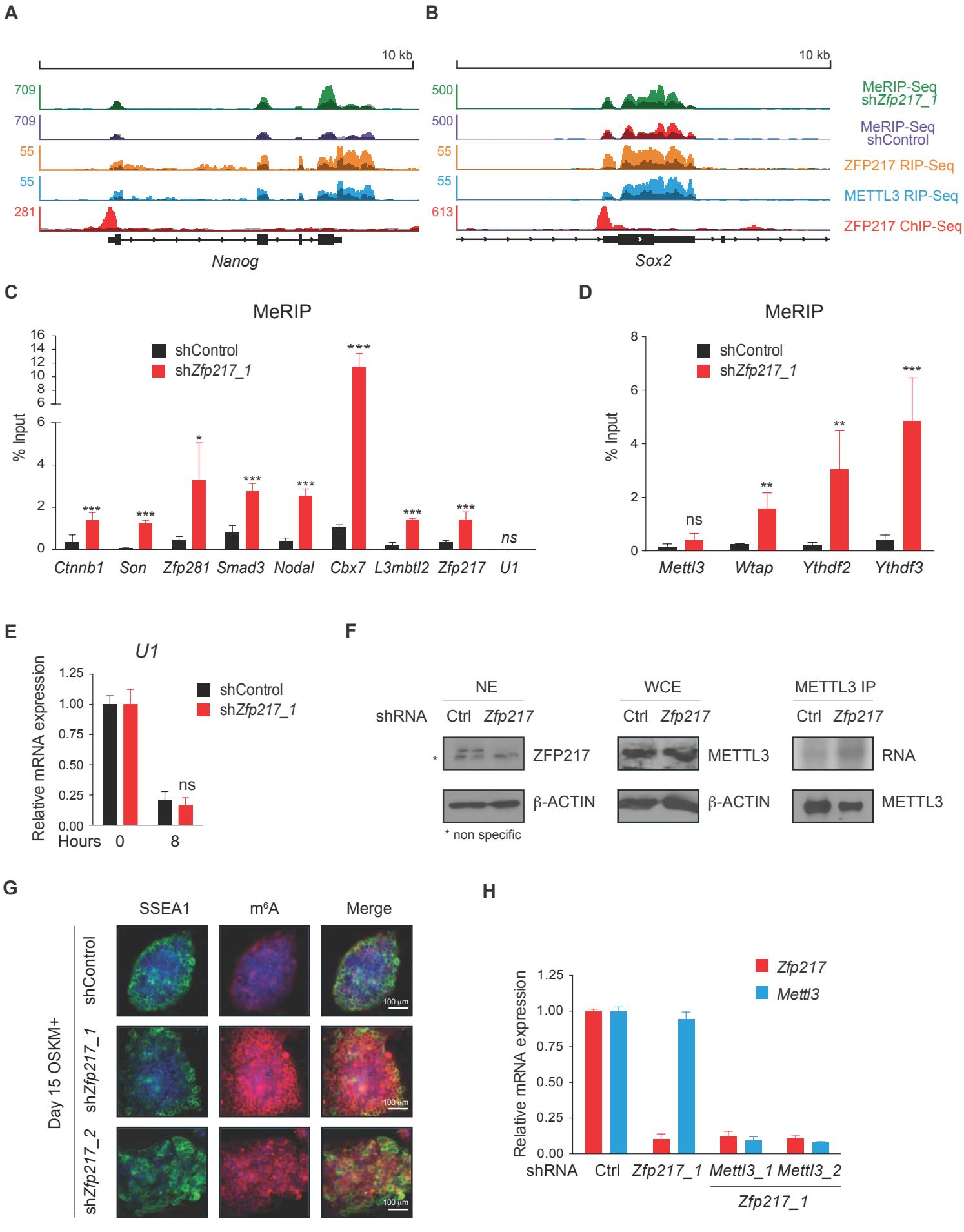
A
10 kb
709
709
55
55
281
Nanog
B
10 kb
500
500
55
55
613
Sox2
MeRIP-Seq shZfp217_1
MeRIP-Seq shControl
ZFP217 RIP-Seq
METTL3 RIP-Seq
ZFP217 ChIP-Seq
C
MeRIP
shControl
shZfp217_1
% Input
Ctnnb1
Son
Zfp281
Smad3
Nodal
Cbx7
L3mbtl2
Zfp217
U1
ns
D
MeRIP
shControl
shZfp217_1
% Input
Mettl3
Wtap
Ythdf2
Ythdf3
ns
E
U1
Relative mRNA expression
shControl
shZfp217_1
ns
Hours 0 8
F
NE
WCE
METTL3 IP
shRNA Ctrl Zfp217
ZFP217
METTL3
RNA
β-ACTIN
β-ACTIN
METTL3
* non specific
G
SSEA1
m6A
Merge
Day 15 OSKM+
shControl
shZfp217_1
shZfp217_2
100 μm
H
Zfp217
Mettl3
Relative mRNA expression
shRNA Ctrl Zfp217_1 Mettl3_1 Mettl3_2
Zfp217_1

SUPPLEMENTAL INFORMATION

Figure S1: ZNF217 mainly functions in later stages of reprogramming, related to Figure 2.

(A) Representative bright field and fluorescence images of MEFs infected with control or *Zfp217* shRNA lentiviruses in the presence of pMX-GFP to monitor infection efficiency.

(B-C) *Zfp217* (B) and *Nanog* (C) mRNA expression in isolated iPSC colonies originated from control and *Zfp217* shRNA transduced reprogramming MEFs. X-axis represents different clones. Results are mean ± SD. Significance of difference compared to control shRNA (***p<0.0001).

(D-O) Representative RT-qPCR analysis of pluripotency (D-G), epithelial (H-K) and mesenchymal genes (L-O) in reprogramming MEFs transduced with control, *Zfp217_1* and *Zfp217_2* shRNAs at day 5, 10 and 15 post-infection. Values are related to MEFs (day 0) as mean ± SD.

Figure S2: Occupancy of ZFP217 at enhancers and core promoters, related to Figure 3.

(A) p300, MED1, H3K4me1 (characteristic of predicted enhancer), H3K27ac (active state) and H3K27me3 (repressed state) occupancy around the summit of ZFP217 peaks.

(B) Pol II Ser-5P and H3K4me3 (characteristic of promoters) occupancy around the summit of ZFP217 peaks.

(C) Venn diagram showing the overlapping between the ChIP-Seq peaks from Pol II Ser-2P, Pol II Ser-5P and ZFP217.

(D) Percentage of REST cofactors (SIN3A/B), REST and CoREST paralogs (RCOR1-3) that co-occupy ZFP217 targets. Anchor set refers to % of ZFP217 peaks whereas partner set refers to the specified transcription factor.

(E) Functional categories of bivalent genes occupied by ZFP217. The p-value for the enrichment of biological process GO-term is shown.

Figure S3: ZFP217, LSD1 and the pluripotency factor POU5F1 overlap in the ESC genome, related to Figure 4.

(A-C) ChIP-Seq binding profiles for LSD1 (green), POU5F1 (blue) and ZFP217 (red) at the *Pou5f1* (F), *Nanog* (G), and *Sox2* locus (H). Input for the ZFP217 ChIP-Seq dataset is depicted in grey. The position of primers used for ChIP-qPCR is shown except for primers used to amplify *Nanog* enhancer 2, which are located at 44.9 kb from the TSS.

(D_G) RT-qPCR analysis of ectodermal (A), trophectodermal (B), mesodermal (C), and endodermal lineage genes (D) in *Zfp217_1* and *Zfp217_2* shRNAs compared to control shRNA. Data are represented as mean ± SD; n = 3. *p<0.005; **p<0.001; ***p<0.0001 versus control shRNA

(H) Venn diagram illustrating the overlapping between LSD1, POU5F1 and ZFP217 ChIP-Seq peaks.

(I) Immunoprecipitation of nuclear extracts from ESCs with ZFP217 or POU5F1 antibodies followed by immunoblotting with ZFP217, LSD1 and POU5F1 antibodies. IgG was used as a control.

(J) Venn diagram showing the overlapping between super-enhancer regions and ZFP217 ChIP-Seq peaks.

Figure S4: METTL3 is not required for ESC pluripotency, related to Figure 5.

(A) Schematics illustrating m^6A methylation and demethylation of RNA with components of the m^6A complex and the YTH family of proteins acting as m^6A 'readers' (*upper panel*). Heat map of the expression of m^6A methylation complex and the YTH family of protein during RA-induced differentiation (*lower panel*). Red and blue indicate increase and decrease of expression, respectively.

(B) RT-qPCR (*upper panel*) and western blot analysis with METTL3 antibodies (*lower panel*) showing the *Mettl3* knockdown efficiency. RT-qPCR data are represented as mean ± SD; n = 3. β-ACTIN was used as a loading control.

(C) Representative images of AP staining of control and *Mettl3*-depleted ESCs.

(D) RT-qPCR analysis of the pluripotency factors *Nanog*, *Pou5f1* and *Sox2* in control and *Mettl3_1* and *Mettl3_2* shRNA infected ESCs. Data are represented as mean ± SD; n = 3; ns= not significant versus control shRNA.

(E) *Mettl3* mRNA (*upper panel*) and METTL3 protein levels (*lower panel*) in control and *Zfp217*-depleted (shRNA 1 and 2) ESCs assessed by RT-qPCR and immunoblotting respectively. Data are represented as mean ± SD; n = 3; ns= not significant versus control shRNA. For the immunoblot, ZFP217 was used to monitor knockdown efficiency and β-ACTIN was used as a loading control.

(F) m^6A immunostaining of ESCs transduced with control or *Zfp217_2* shRNAs. Nuclei were stained with DAPI. The scale bar represents 100 μ m

(G) Dot blot analysis of polyadenylated RNA (poly(A)$^+$) isolated from control and *Zfp217_2* shRNA ESCs. Indicated amounts were loaded and detected with m^{6}A antibody. Methylene blue staining was used as a loading control.

(H-I) LC-MS/MS quantification of the m^{6}A/A ratio in polyadenylated RNA isolated from control and *Zfp217_2* (H) or *Mettl3* knockdown ESCs (I). Error bars show ± SD; n = 3. **p<0.001; *p<0.005 versus control shRNA.

Figure S5: ZFP217 and METTL3 transcriptomes overlap, related to Figure 6.

(A) Normalized distribution of control and *Zfp217* shRNA m^{6}A peaks across the 5'UTR, CDS, and 3'UTR of mRNAs.

(B) Length distribution of internal exons of m^{6}A transcripts identified in control and *Zfp217* shRNA.

(C) Scatter plot of the expression of m^{6}A transcripts in control compared to *Zfp217*-depleted ESCs.

(D) Pie chart showing the distribution of the diverse class of RNAs bound by ZFP217 (*left*) and METTL3 (*right*).

(E-F) Functional categories of ZFP217 (E) and METTL3-bound transcripts (F). The p-value for the enrichment of biological process GO-term is shown.

(G) Diagram illustrating the coverage across gene bodies of genes containing both ChIP and RIP peaks or ChIP peaks only with ZFP217 antibodies.

(H-I) Coverage of RNA pol II (H) and POU5F1 (I) signal at the TSS of modified and unmodified genes.

Figure S6: ZFP217 regulates different layers of pluripotency, related to Figure 7.

(A-B) Binding profiles depicting MeRIP-Seq for *Zfp217* (green) and control shRNA (purple), RIP-Seq for ZFP217 (orange) and METTL3 (blue), and ZFP217 ChIP-Seq (red) at *Nanog* (F) and *Sox2 locus* (G). Input is shown in grey.

(C-D) MeRIP analysis of transcripts with a known function in ESC biology (*see* **Table S6**) (C) and m^{6}A metabolism (D) in control and *Zfp217*-depleted ESC. Percentage of input is shown. Data are represented as mean ± SD; n = 3. ***p<0.0001; **p<0.001; *p<0.01; ns= not significant versus control shRNA.

(E) RT-qPCR analysis of *U1* after 8 hours of EU incorporation in control and *Zfp217* shRNA ESCs. Data are represented as mean ± SD; n=2. ns= not significant versus control shRNA at 8 hours.

(F) PAR-CLIP of METTL3 in control and *Zfp217*-depleted ESC. Endogenous METTL3 protein-RNA complex was pulled down with METTL3 antibodies, and the RNA was labeled with [γ-32-P]-ATP and visualized by autoradiography. The levels of METTL3 protein in whole cell lysate (WCE) and knockdown efficiency of *Zfp217* in nuclear extracts (NE) were detected by western blotting with specific antibodies. β-ACTIN was used as loading control.

(G) SSEA1 and m^6A immunostaining of reprogramming MEFs 15 days after transduction with Control, *Zfp217_1* or *Zfp217_2* shRNAs. Nuclei were stained with DAPI. The scale bar represents 100 μ m.

(H) RT-qPCR analysis of *Zfp217* and *Mettl3* showing the knockdown efficiency with the indicated shRNAs at day 15 of reprogramming.

SUPPLEMENTAL TABLES

Table S1, related to Figure 3: ChIP-Seq for ZFP217 and RNA-Seq upon knockdown of *Zfp217* in mouse ESCs. See separate excel File, Table S1.xlsx

Table S2, related to Figure 4: RNA-Seq. Gene expression during differentiation of ESCs with retinoic acid (from day 0 to day 6). Fold-change is shown. See separate excel File, Table S2.xlsx

Table S3, related to Figure 5: Mass spectrometry of ZFP217-interacting proteins. Columns indicate name, accession number, spectra, number of unique peptides obtained, coverage, known role in ESC biology, known role in RNA metabolism and described function. *Indicates previously described ZFP217 interaction.

Name	Accession Number	Spectra	Uniq Peptides	Coverage	Function in ESC	Function in RNA	Function
LSD1*	Q6ZQ88	11	8	13.6	x		Histone demethylase
METTL3	Q8C3P7	2	1	10.2	x	x	m^6A methyltransferase
RBPMS2	Q9WVB0	2	2	13.2		x	RNA recognition motif (RRM) family
HIST1H2P	Q8CGP2	1	1	7.1		x	Core component of nucleosome
RCOR1*	Q8CFE3	3	3	9.2	x		Corepressor
RPS3	P62908	1	1	6.1		x	S3P family of ribosomal proteins
CTBP1*	O88712	2	2	4.3	x		Corepressor
HDAC1*	O09106	2	2	4.4	x		Histone deacetylase
RCOR2*	Q8C796	2	2	3.6	x		Corepressor
NPM1	Q61937	1	1	4.8	X (HSC)	x	Multifunctional nucleolar protein
NAT2	P50295	1	1	16.2			N-acetyltransferase 2
CTBP2*	P56546	1	1	7.4		x	Corepressor
EIF3G	Q9Z1D1	1	1	2.8		x	Initiation of protein synthesis
TRMT10C	Q3UFY8	1	1	3.4		x	tRNA methyltransferase 10C
SF3B4	Q8QZY9	1	1	3.3		x	Splicing
ACVR2A	P27038	1	1	3.7		x	Modulation of TGFb signals

ZFP217	Q3U0X6	2	2	2.7	this paper	this paper	BAIT
IWS1	Q8C1D8	1	1	1.4		x	RNAPII elongation complex
THRAP3	Q569Z6	1	1	1.1		x	Transcriptional coactivation
BCL-2	Q8K019	1	1	1			Cell death
DHX9	O70133	1	1	0.9		x	RNA helicase
NIPBL	Q6KCD5	2	1	0.6	x		Structural role in chromatin

Table S4, related to Figure 6: MeRIP-Seq. Genes with lower and higher m^6A peaks in *Zfp217* knockdown compared to control. See separate excel File, Table S4.xlsx

Table S5, related to Figure 6: RIP-Seq for ZFP217 and METTL3 immunoprecipitated from mouse ESCs. See separate excel File, Table S5.xlsx

Table S6, related to Figure 7: List of m^6A ZFP217-dependent transcripts that overlap with ZFP217 ChIP-Seq, ZFP217 and METTL3 RIP-Seq datasets, and have a known function in ESC biology.

Gene	Reference
β–catenin (*Ctnnb1*)	(Clevers, 2006)
Son	(Lu et al., 2013),
Zfp281	(Fidalgo et al., 2012; Fidalgo et al., 2011; Wang et al., 2008)
Smad3	(Brown et al., 2007)
Nodal	(Ogawa et al., 2007)
Cbx7 (PRC1)	(Morey et al., 2012; O'Loghlen et al., 2012)
L3mbtl2 (PRC1)	(Qin et al., 2012)
Zfp217	This paper

Table S7, related to experimental procedures: RT-qPCR primers used for gene expression analysis, ChIP validation, MeRIP validation, and cloning of genomic regions into luciferase vector. See separate excel File, Table S7.xlsx

SUPPLEMENTAL EXPERIMENTAL PROCEDURES

Antibodies

The following commercially available antibodies were used at the indicated concentrations for western blot: anti–β-ACTIN (Sigma, A5441, 1:1,000), anti-OCT4 (Abcam, ab19857, 1:1,000), anti-NANOG (Bethyl, catalogue number A300-397A, 1:1000), anti-SOX2 (Santa Cruz, sc-17320, 1:1,000), anti-LSD1 (Abcam, ab17721, 1:1,000), anti-METTL3 (Bethyl, A 301-567A, 1:1,000), and anti-METTL14 (Aviva Systems Biology, ARP50652_P050). ZFP217 rabbit polyclonal antibody was kindly provided by Dr. Sheryl Krig (Huang et al., 2005). Protein A HRP (Abcam, ab7456, 1:1,000) was used for westernblot detection of METTL14. ChIP analysis was performed with the indicated amount of

specified antibodies and number of cells: anti-ZNF217 (C-17) (Santa Cruz, sc 55351x; 5 μg antibody for 1 x 10^7 cells), anti-OCT3/4 (N-19) (Santa Cruz, sc-8628; 5 μg antibody for 5 x 10^6 cells) and anti-LSD1 (Abcam, ab17721, 1:1,000; 10 μg antibody for 1 x 10^7 cells). Co-IP experiments were performed with the same antibodies and amounts as for ChIP, including anti-METTL3 (Bethyl, A 301-567A, 3 μg antibody for each IP). For IF analysis of iPSC, E-CADHERIN (Takara, catalogue number M108, 1:400), SSEA1 (BD Pharmigen, catalogue number 561560, 1:400), NANOG (Bethyl, catalogue number A300-397A, 1:500) and m^6A antibodies (Synaptic Systems, catalogue number 202 003, 1:250) were used. Dot-blot (1:1,000) and MeRIP experiments (4.5 μg antibody for each IP) were performed with m^6A antibody.

Cell culture and differentiation assays

The mouse ESC line CCE was maintained on 0.1% gelatin-coated tissue culture plates under feeder-free culture conditions. ESC media includes: D-MEM high glucose (Dulbecco's modified Eagle's medium 1× high glucose), 15% FBS (fetal bovine serum; Hyclone), 100 mM MEM non-essential amino acids, 0.1 mM 2-mercaptoethanol, 1 mM L-glutamine and penicillin/streptomycin (Invitrogen) and 10^3 units ml^{-1} Leukemia inhibitory factor (LIF) (eBioscience). To induce differentiation with retinoic acid (RA), LIF (eBioscience) was removed and RA (Sigma-Aldrich) was added at a concentration of 5 μM. EBs were obtained by growing ESCs in low-attachment dishes in the presence of complete medium and without LIF. Medium was changed every other day. Cells and EBs were harvested for extraction of total RNA at the indicated time points. All cell cultures were maintained at 37 °C with 5% CO_2.

Cell somatic reprogramming

For reprogramming experiments, early passage MEFs were seeded at a density of 50,000 cells in 6-well plates and infected with a single lentiviral stem cell cassette (STEMCCA), constitutively expressing all four Yamanaka factors (OCT4, KLF4, SOX2, c-MYC; OKSM). The day after infection, MEFs were replated at a density of 50,000 cells/ well on irradiated MEF feeder layers and cultured in mouse iPSC media, containing high-glucose DMEM supplemented with 15% KnockOut Serum Replacement (Invitrogen), 100 mM MEM non-essential amino acids, 1 mM L-glutamine, 0.1 mM β-mercaptoethanol, 100 units/mL penicillin/streptomycin, 1 mM sodium pyruvate and 1000 U/mL LIF. Media was changed every day. Alternatively, MEFs were infected with OKSM in the presence of different constructs: shRNA control, shRNA *Zfp217_1*, shRNA *Zfp217_2*, shRNA *Mettl3_1*, shRNA *Mettl3_2*, or combination of shRNA control or shRNA *Zfp217_1* with shRNA *Mettl3_1* or shRNA *Mettl3_2*. For overexpression experiments MEFs were infected with OKSM and pSIN-EF2-HA or

pSIN-EF2-HA-ZFP217. Reprogramming MEFs were examined by AP staining, immunofluorescence microscopy, and RT-qPCR at the indicated days post-infection.

Alkaline phosphatase activity and Immunofluorescence staining

Alkaline phosphatase activity was measured using the Stemgent Alkaline Phosphatase Staining kit (Stemgent), following the manufacturer's recommendations. For immunofluorescence staining, cells were fixed in 4% paraformaldehyde (PFA) at room temperature (RT) for 15 min, followed by permeabilization at RT for 5 min with 0.25% Triton-X-100 in PBS. Cells were then washed twice with PBS and blocking was performed at 37 °C for 30 min with 10% BSA in PBS. The cells were stained with the specified antibodies overnight at 4 °C in 3% BSA in PBS. Images were acquired using a LEICA DMI6000 B microscope.

Cellular proliferation, apoptosis assay and cell cycle analyses

Cellular proliferation, apoptosis assay and cell cycle analysis were performed utilizing Muse™ Cell Analyzer from Millipore (Billerica, MA) following manufacturer's instructions.

Nuclear extracts extraction

Cells were expanded to 150 mm diameter tissue culture plates, washed with cold PBS, and scraped off, and nuclear extracts were prepared as previously described with some modifications (Dignam et al., 1983). Briefly, cellular pellet was resuspended in at least 5 volumes of buffer A (10 mM HEPES pH 7.9, 1.5 mM $MgCl_2$, 10 mM KCl, 1 mM DTT) in the presence of protease inhibitors (3 µg/ml aprotinin, 750 µg/ml benzamidine, 1 mM phenylmethylsulfonyl fluoride, 5 mM NaF and 2 mM sodium orthovanadate) and incubated for 10 minutes in ice. Following centrifugation, the pellet was resuspended in 2 volumes of buffer A, Douncer-homogenized, and spun down at maximum speed for 5 minutes. Nuclei were then resuspended in 2 volumes of buffer B (20 mM HEPES pH 7.9, 1.5 mM $MgCl_2$, 500 mM NaCl, 25% Glycerol, 0.5 mM EDTA, 1 mM DTT) supplemented with protease inhibitors and incubated in a rotator at 4 degrees for 30 minutes. Finally, the samples were spun down at maximum speed for 15 minutes and frozen at -80 ^{o}C for further analysis.

Co-immunoprecipitation and immunoblotting

For immunoprecipitation experiments, 500 µg of nuclear extracts were pre-cleared with protein G agarose (Roche) for 1 hr and incubated overnight with specific antibodies at 4 ^{o}C. The day after, protein G beads were added for 2 hours before washing 4 times in ice-cold Nonidet P-40 buffer (20 mMTris HCl pH 8, 137 mM NaCl, 1% Nonidet P-40 (NP-40), 2 mM EDTA) supplemented with protease inhibitors. Where indicated, RNase A (100 µg/ml; 1 hour at 4 ^{o}C) or DNase I (40 U/ml; 20 min

at 37 °C) were added before the immunoprecipitation procedure. DNase I was inactivated with 10 mM EDTA treatment before IP. Immunoprecipitated complexes were resolved by SDS-PAGE, transferred to PVDF membranes (Bio-Rad), and immunoblotted with the indicated antibodies followed by ECL detection (Thermo Scientific).

Lentiviruses generation and mouse ESC transduction

All shRNAs used in this study are listed below:

Plasmid	shRNA sequence
pLKO.pig Luc shRNA	CTTACGCTGAGTACTTCGA
pLKO.1-puro-scr	CAACAAGATGAAGAGCACCAA
pLKO.pig.Znf217_1 shRNA	CCGGCACACTTCCACGGAATCATACCTCGAGGTAT GATTCCGTGGAAGTGTGTTTTTG
pLKO.pig.Znf217_2 shRNA	CCGGTCACATCAGCACCTATCTAACCTCGAGGTTA GATAGGTGCTGATGTGATTTTTG
pLKO.pig Nanog shRNA	GCCAACCTGTACTATGTTTAA
pLKO.pig Oct4 shRNA	GCGAACTAGCATTGAGAAC
pLKO.pig Sox2 shRNA	GGTTGATATCGTTGGTAAT
pLKO.1-puro-Mettl3_1 shRNA	CGTCAGTATCTTGGGCAAATT
pLKO.1-puro-Mettl3_2 shRNA	GGAGATCCTAGAGCTATTAAA

pLKO-based shRNAs targeting *Pou5F1*, *Nanog* and *Sox2* were kindly provided by Dr. Lemischka (Icahn School of Medicine at Mount Sinai, New York). Lentiviral pLKO-based shRNA targeting *Mettl3* were kindly provided by Dr. Zhao (Sanford Burnham, La Jolla, California). Lentiviruses were generated in HEK-293T cells by Lipofectamine-mediated cotransfection of lentiviral-based shRNA plasmids and the pCMV-dR8.2 (packaging) and pCMV-VSVG (envelope) plasmids. Virus supernatants were concentrated using Amicon Ultra centrifugal filter units (Millipore) at 1600g for 20 min., and stored at -80 °C. For infection, ESCs were transduced with virus in media supplemented with polybrene (10 μg/ml). Cells were incubated overnight with virus and subsequently cultured in fresh media for 4 days. After 4 days, cells were cultured in media supplemented with 1 μg/mL puromycin for 4 additional days.

RT-qPCR analysis

RNA was extracted using Trizol and the RNeasy Mini Kit (Qiagen). One to five μg total RNA was reverse transcribed using the PrimeScript RT Reagent kit (Takara). Alternatively, the SuperScript® VILO™ cDNA Synthesis Kit (Life Technologies) was used for low amount of RNA input. Quantitative PCR was performed using the GoTaq® qPCR Master Mix (Promega) on the Stratagene Mx3005P

Real-Time PCR System (Agilent Technologies). Gene expression specific primers used for this study are listed in Table S7. *Beta-actin* mRNA was assayed as loading control.

Generation and Expression of Luciferase Expression constructs.

A minimal *Oct4* promoter was amplified from mouse genomic DNA and cloned into the XhoI and HindIII sites of the pGL3 basic vector (Promega) with In-Fusion® Cloning Technology (Clontech). Enhancer fragments were amplified from mouse genomic DNA, and subsequently cloned into the BamHI and SalI sites of the pGL3-*pOct4* vector. All primers used are listed in Table S7. 100 ng of the plasmids were used to transfect $2x10^5$ CCE cells depleted of *Zfp217* (shRNA 1 and shRNA 2) or cells control in 24-well plates using Lipofectamine LTX (Invitrogen) according to the manufacturer´s instructions. 5 ng of the pRL-CMV plasmid was co-transfected in each well as a normalization control. Cells were incubated for 48 hours, and luciferase activity was measured using the Dual-Luciferase Reporter Assay System (Promega). Luciferase activity was normalized to the activity measured in cells transfected with a construct containing only the *Oct4* promoter. Experiments were performed in duplicates.

Chromatin immunoprecipitation with high-throughput sequencing (ChIP-Seq)

ChIP experiments were performed as described (Marson et al., 2008) with slight modifications. Cells were chemically crosslinked by the addition of 1/10 volume of fresh 11% formaldehyde solution for 10 minutes at RT followed by addition of glycine 1/20 volume of 2.5 M for 5 min at RT. After rinsing twice with ice-cold PBS, cells were collected by centrifugation, and lysed in the following buffers for 10 min at 4 ^{o}C: Lysis buffer 1 (50 mM, Hepes-KOH (pH 7.5), 140 mM NaCl, 1 mM EDTA, glycerol (10% vol/vol) NP-40 (0.5% vol/vol), Triton X-100 (0.25% vol/vol)) and Lysis buffer 2 (200 mM NaCl, 1 mM EDTA, 0.5 mM EGTA, 10 mM Tris (pH 8)) with complete protease inhibitors (Roche). To solubilize and shear crosslinked DNA, cells were sonicated in lysis buffer 3 (100 mM NaCl, 1 mM EDTA, 0.5 mM EGTA, 10 mM Tris (pH 8), Na-Deoxycholate (DOC) (0.1% vol/vol), N-lauroyl sarcosine (0.5% vol/vol)) for 30 x 30 second pulses (30 second pause between pulses) at high power in a Bioruptor® Sonication System (Diagenode). The resulting whole cell extract was incubated overnight at 4°C with 50 µl of Dynabeads® Protein G magnetic beads and the indicated amount of antibody. Protein-DNA complexes were washed 4-5 times with RIPA buffer (50 mM Hepes (pH 7.6), 1mM EDTA, DOC (0.7% vol/vol), NP-40 (1% vol/vol), 0.5M LiCl) and once with TE containing 50 mM NaCl, and eluted from the beads twice by incubation with 100 µL of elution buffer (50 mM Tris (pH 8), 10 mM EDTA, SDS (1% vol/vol) by heating at 65°C with occasional vortexing for 15 minutes. Crosslinking was reversed by adding 200 mM NaCl and incubating at 65°C overnight. Input sample was also treated for crosslink

reversal. Samples were treated with RNase A and proteinase K as manufacture's recommendations. DNA was purified by phenol–chloroform extraction, followed by ethanol precipitation. Fold enrichment over 10% input was calculated using the 2DeltaCt method. The primer sets used for ChIP analysis are listed in Table S7.

Library preparation

ChIP-Seq libraries were prepared according to the NEBNext ChIP-Seq Library Prep Master Mix Set for Illumina (NEB) protocol. Briefly, ChIP DNA was end-repaired, A-tailed, Illumina adaptors were ligated, and the DNA separated on a 2% agarose gel. DNA fragments of 200 bps were excised and purified using a QIAquick Gel Extraction Kit (Qiagen). Size-selected DNA was amplified with 16 PCR cycles and further purified with Agencourt Ampure XP beads (Beckman Coulter). Quality control and quantification of the library were assessed in an Agilent Bioanalyzer (Agilent Technologies, Inc.). Sequencing of multiplexed DNA libraries was done on Illumina HiSeq 2500 following the manufacturer's instructions.

ChIP-Seq analysis

After QC filtering by FASTX (http://hannonlab.cshl.edu/fastx_toolkit/), only the reads with a quality score Q20 in at least 90% bases were included for the analysis. ChIP-Seq reads were aligned to the mouse reference genome (mm9, NCBI build 37) using the software Bowtie2 (Langmead and Salzberg, 2012). ZFP217 ChIP-Seq peaks were called by MACS2 algorithm (Zhang et al., 2008), and subsequently annotated with genome mapping information of RefSeq transcripts. Genes with enriched regions within 5kb of their transcription start site were considered ZFP217-bound.

ChIP-Seq signal tracks were presented by Integrative Genomics Viewer (IGV) software (http://www.broadinstitute.org/igv/). ZFP217 *de-novo* motif analysis and transcription factor binding sequence motifs enriched in ZFP217 peak sequences were obtained with MEME-ChIP software (http://meme.nbcr.net/meme/cgi-bin/meme-chip.cgi) (Machanick and Bailey, 2011).

To perform the ChIP-Seq density heat maps, selected enriched regions were aligned with each other according to the position of the TSS. For each experiment, the ChIP-Seq density profiles were normalized to the density per million mapped reads. To examine chromatin patterns, enrichment profiles around ZFP217 binding peaks with previously reported ESC ChIP-Seq datasets for p300, MED1, mono methylated histone H3 Lys4 (H3K4me1), characteristic of predicted enhancer, and acetyl histone H3 Lys27 (H3K27ac) and tri-methylated histone H3 Lys27 (H3K27me3), marking activated and repressed states, respectively were generated (**Figure S2A**) (Arnold et al., 2013; Heintzman et al., 2009; Heintzman et al., 2007; Rada-Iglesias et al., 2011; Visel et al., 2009). To

detect promoter occupation, ChIP-Seq enrichment profiles of RNA polymerase II Ser-5 phosphorylated (Pol II Ser-5P) and the histone modification tri-methylated histone H3 Lys4 (H3K4me3) with high-confidence ZFP217 peaks (**Figures S2B** and **S2C**) were also clustered. Each gene in the mouse genome was also classified into (i) active, containing H3K4me3 at the TSS and di-methylated histone H3 Lys 79 (H3K79me2) within the first 5 Kb of the gene body; (ii) bivalent or poised, associated with H3K4me3 and H3K27me3 at the TSS and (iii) silent, associated with the absence of H3K4me3 and H3K79me2 and the possibility to contain H3K27me3, and overlapped the ZFP217-bound peaks (**Figure 3G**).

Below is the list of ChIP-Seq datasets used, corresponding GEO Accession numbers and publication:

Datasets	GEO Accession Number	Publication
POU5F1	GSM566277	(Ang et al., 2011)
LSD1	GSM687282	(Whyte et al., 2012)
p300	GSM918750	(2012; Yue et al., 2014)
MED1	GSM560347, GSM560348	(Kagey et al., 2010)
H3K4me1	GSM769009	(Yue et al., 2014)
H3K27ac	GSM594578, GSM594579	(Creyghton et al., 2010)
Pol2 ser-5	GSM515662	(Rahl et al., 2010)
Pol2 ser-2	GSM515663	(Rahl et al., 2010)
H3K4me3	GSM769008, GSE11724	(Marson et al., 2008; Yue et al., 2014)
H3K79me2	GSE11724	(Marson et al., 2008)
H3K27me3	GSM1000089, GSM307619	(Mikkelsen et al., 2007; Yue et al., 2014)
REST	GSM698696	(Yu et al., 2011)
SIN3A	GSM698700	(Yu et al., 2011)
SIN3B	GSM698701	(Yu et al., 2011)
RCOR1	GSM698697	(Yu et al., 2011)
RCOR2	GSM698698	(Yu et al., 2011)
RCOR3	GSM698699	(Yu et al., 2011)

RNA-Seq library preparation

RNA-Seq library preparation was performed at the Weill Cornell Medical College Genomic Core facility (New York) using the TrueSeq RNA sample preparation kit (Illumina RS-122-2001) as per manufacturer's recommendations. Samples were sequenced by the Illumina HiSeq 2500 platform (Illumina) as 100 bp pair-ended reads.

RNA-Seq analysis

Contaminant (aligned) RNA-Seq reads was filtered and aligned to several mouse reference databases including the mouse genome (mm9, NCBI Build 37), RefSeq exons and splicing junctions using BWA alignment algorithm (http://bio-bwa.sourceforge.net/) (Li and Durbin, 2010). The reads that were uniquely aligned to the exon and splicing-junction sites for each transcript were then counted as

expression level for a corresponding transcript and were subjected to log2 transformation and global median normalization. Differentially expressed genes were identified by the R package DEGseq (Wang et al., 2010) using a false discovery rate (FDR) < 0.001 and fold-change >1.5.

PAR-CLIP

PAR-CLIP experiments were performed as previously reported (Spitzer et al., 2014) with some modifications. Briefly, CCE cells were incubated with 200 μM of 4SU (Sigma Aldrich) for 14 hrs and were crosslinked with 0.4 J cm^{-2} at 365 nm. After lysis, immunoprecipitation was carried out with ZFP217 or METTL3 antibodies (5 μg and 3 μg, respectively) over night at 4 °C. Precipitated RNA was labeled with [γ-32-P]-ATP and visualized by autoradiography. One third of the sample was separated by SDS-PAGE to detect ZFP217 or METTL3 immunoprecipitation efficiency. The relative density of RNA bound by METTL3 was analyzed by Image Studio Lite software. For PAR-CLIP-RT-qPCR analysis, proteins were removed with Proteinase K digestion, RNA was extracted using Trizol and the RNeasy Mini Kit (Qiagen), and RNA was reverse transcribed with SuperScript® VILO™ cDNA Synthesis Kit. RT-qPCR analysis of the retrotranscribed RNA was performed with specific primers as indicated.

RNA immunoprecipitation (RIP)-Seq

RNA immunoprecipitations were performed with RNA ChIP-IT® Magnetic Chromatin Immunoprecipitation kit (Active Motif) following the manufacturer's protocol. RIP-Seq library preparation was performed at the Weill Cornell Medical College Genomic Core facility (New York) using the TrueSeq RNA sample preparation kit (Illumina RS-122-2001) skipping the polyA tail purification step. Libraries were sequenced by the Illumina HiSeq 2500 platform (Illumina) as 100 bp pair-ended reads.

After filtering contaminant (aligned) RIP-Seq reads, TopHat 2.0.8 alignment software (Trapnell et al., 2009) via Bowtie (Langmead et al., 2009) was used to align the RIP-Seq reads to the mouse reference genome (mm9, NCBI Build 37) and genes were annotated with Gene Transfer Format (GTF) of Ensembl. The Cufflinks/Cuffdiff suite (Trapnell et al., 2010) was used to compute the fragments per kilobase of exon per million fragments mapped (FPKM) values as means of normalizing for gene length and depth of sequencing, and the fold-change difference of gene expression in terms of FPKM between the RIP and control (input) libraries. Transcripts were considered detected if their FPKM expression > 1.0 and the ratio of FPKM[RIP]/FPKM[input] > 1.5.

N^6-methyladenosine (m^6A) RIP-Seq

m^{6}A immunoprecipitation was performed as described elsewhere (Dominissini et al., 2013). Briefly, 300 μg of total RNA were fragmented using a RNA fragmentation kit (New Englands Biolabs), and incubated with 4.5 μg anti-m^{6}A antibody (Synaptic Systems) in RIP buffer (750 mM NaCl, 50 mM Tris-HCl (pH 7.4) and 0.5% (vol/vol) NP40) supplemented with RNasin (40 U/ μl) and 2 mM RVC for 2 h at 4 °C, followed by the addition of washed protein A agarose beads (Roche) and further incubation at 4 °C for 2 h. Beads were washed 3 times in RIP buffer and incubated twice with 100 μl immunoprecipitation buffer containing 6.7 mM m^{6}A (Chem-Impex International, Inc) at 4 °C for 1 h to elute RNA. Immunoprecipitated RNA was extracted with phenol/chloroform and samples were sent to Weill Cornell Medical College Genomic Core facility (New York) for library construction. Samples were sequenced by the Illumina HiSeq 2500 platform (Illumina) as 50 bp pair-ended reads. Alternatively, immunoprecipitated RNA was resuspended in 32 μl of water and 14 μl were reversed transcribed using the SuperScript® VILO™ cDNA Synthesis Kit (Life Technologies) and RT-qPCR was performed with primers listed in Table S7.

Analysis of m^{6}A MeRIP-Seq datasets

Analysis of the m^{6}A MeRIP-Seq data was conducted as previously described (Dominissini et al., 2013). Briefly, read sequences were filtered by the FASTQC tool (http://www.bioinformatics.babraham.ac.uk/projects/fastqc/) and then aligned to the mouse reference genome (mm9, NCBI Build 37) with Bowtie2 software (Langmead et al., 2009). The peak-caller MACS version 1.4 (Zhang et al., 2008) was used for peak detection with the following parameters: (i) the "effective genome size" was adjusted to the calculated transcriptome size (1.75*108), according to the UCSC table browser, (ii) the size of input RNA fragments was set to 50 nt, and (iii) p-value cutoff was set to 1.00e-05. MACS-identified peaks were sorted according to their fold change and the top 1,000 peaks falling within known RefSeq genes were chosen for *de novo* motif analysis. 101-nucleotide-long sequences derived from the sense strand and centered on the peak summit were used as input for MEME (http://meme.nbcr.net/meme/cgi-bin/meme.cgi) (Machanick and Bailey, 2011). For the motif analysis of ZFP217-dependent m^{6}A peaks, the following criteria was applied: (i) control and *Zfp217* shRNA peaks had to be detected by MACS (and filtered by fdr <0.01, fold enrichment > 5) and increased in *Zfp217* shRNA compared to control shRNA according to exomePeak tool; (ii) the 100bp region around the summit was used as input for MEME. CentriMo (http://meme.nbcr.net/meme/cgi-bin/centrimo.cgi) (Bailey and Machanick, 2012) was applied to generate the density curves of the consensus motif at positions flanking the summit of control and *Zfp217* shRNA peaks. m^{6}A peaks were annotated with by applying PeakAnalyzer (http://www.ebi.ac.uk/research/bertone/software)

(Salmon-Divon et al., 2010).

To study the peak distribution on transcripts, only one transcript variant of each gene of the RefSeq gene annotation was taken in consideration. 10 bins of equal length were made for 5'UTR, CDS 3'UTR respectively and intersectBed tool was used to calculate the number of peaks that mapped to each bin. Then the bins were plotted as a percentage of the total number of peaks in the dataset.

Gene Ontology (GO) Analysis

For functional profiling of ZFP217 binding regions identified by ChIP-Seq that overlapped with POU5F1 and LSD1 peaks (**Figure 4E**), gene ontology analysis was performed using GREAT v. 1.2.6 (http://bejerano.stanford.edu/great/public/html/) (McLean et al., 2010) with the single nearest gene regulatory definition option. For Figures 3C, 3D, 6B, 7B and supplemental Figures 2E and 5B, gene ontology analysis was performed using the web tool The Database for Annotation, Visualization and Integrated Discovery (DAVID) (http://david.abcc.ncifcrf.gov/) (Huang da et al., 2009a, b). Pathway analysis of ZFP217-interacting proteins was performed using ingenuity pathway analysis (IPA; Ingenuity Systems, www.ingenuity.com).

Gene set enrichment analyses

GSEA analysis was performed with GSEA software (http://www.broadinstitute.org/gsea/index.jsp), using RA differentiation gene sets from our study (Table S2) and EB differentiation gene set from previous studies (GSE3749) (Hailesellasse Sene et al., 2007). GSEA results are considered significant when the FDR q-value is less than 0.25 and nominal (NOM) p-value is less than 0.05.

Heat maps

Heat maps were made using Z-score which was calculated as following:

Z=(X-Xav)/Xsd, where X is the log2-transformed expression level for a given gene in a specific sample, Xav is the mean of log2-transformed expression values for that gene in all samples, and Xsd is the standard deviation of log2-transformed expression values for that gene across all samples.

Poly(A)$^+$ RNA selection

Poly(A)$^+$ RNA selection was performed using Poly(A) Purist Magnetic Kit (Life Technologies) according to the manufacturer's protocol.

Dot blots

Indicated amounts of mRNA were mixed 1:1 with denaturation buffer (10 ml deionized formamide, 3.5 mL 37% formaldehyde and 2 mL 5x MOPS) for 5 min at 65 C. Nylon membrane (Nytran N, Schleicher

& Schuell) was hydrated in 10X SSC and then "sandwiched" in Minifold 1 Filtration Manifold (Schleicher & Schuell). Each well was filled with 200 μl of 10x SSC buffer and flushed by gentle suction vacuum twice. After applying the RNA samples, wells were washed with 10x SSC twice. The apparatus was disassembled and the membrane was crosslinked in a UV STRATALINKER 1800 using default settings. After blocking for 1h using sterile RNAse DNase free PBST + 5% milk, the membrane was incubated with m^6A primary antibody (Synaptic Systems, Cat. #202 003, 1:1000) overnight at 4°C. The membrane was then washed four times in PBST and incubated with the secondary anti rabbit antibody (1:5000 dilution) for 1h at RT. The membrane was washed again in PBST and exposed on an auto radiographic film using enhanced chemiluminescence substrate (ECL; GE Healthcare). RNA levels were normalized with methylene blue staining.

Quantitative analysis of m^6A level using LC-MS/MS

Enzymatic hydrolysis of RNA to ribonucleosides was carried out as described previously (Wang et al., 2014). Briefly, 200-300 ng of poly(A)$^+$ RNA were digested with 2 U nuclease P1 (Sigma Aldrich, St. Louis, MO) at 37 ºC for 2 h in 25 μl of buffer containing 25 mM of NaCl and 2.5 mM of $ZnCl_2$, followed by the addition of NH_4HCO_3 (1 M, 3 μl) and alkaline phosphatase (0.5 U) for 2 h at 37 °C. The digestion mixture was diluted to 40 μL using deionized water and centrifuged at 10,000 rpm for 5 min to remove any solid material. 10 μl of the solution was injected into the LC-MS/MS system as described by (Jia et al., 2011). A and m^6A were separated by reverse phase ultra-performance liquid chromatography (UPLC) on a C18 column (HSS T3, 1.7 μm, 2.1 x 100 mm, Waters, Milford, MA), coupled to an electrospray quadrupole-time-of-flight (QSTAR XL, Applied Biosystems, Foster City, CA) mass spectrometer acquiring in positive ionization mode. The product ion scans of the protonated A at *m/z* 268 and m^6A at *m/z* 282 were acquired and the ion fragmentogram for each nucleoside was constructed using the MultiQuant software (Applied Biosystems, Foster City, CA), corresponding to the following precursor ion to product ion transitions: 268 to 136 for A and 282 to 150 for m^6A, was constructed. The Quantification was carried out using a standard curve generated from pure A and m^6A standards (500-3000 nM for A and 1-100 nM for m^6A) ran during the same batch of the samples and injected three times. The ratio of m^6A to A was determined from the calculated concentrations.

Assay to determine RNA stability

To monitor RNA synthesis, cells were incubated with 0.2 mM 5-ethynyl uridine (EU) in growth medium for 16 hours and total RNA was extracted 0 and 8 hours after removal of EU from the culture medium. EU-labeled RNAs were biotinylated and captured using the Click-iT Nascent RNA Capture Kit

according to manufacturer's instructions (Invitrogen), followed by reverse transcription and RT-qPCR analysis. RNA stabilities of several mRNAs were determined relative to *β-actin* mRNA.

Mass Spectrometry analysis to identify the ZFP217 associated protein complexes

10 μg of ZFP217 antibody were conjugated to 0.5 mg of Dynabeads® M-270 Epoxy following the manufacture's instructions (Invitrogen). Then, 600 μg of nuclear extracts were incubated with antibody-coupled beads for 5h at RT. After washing 4 times with NP40 buffer, immunoprecipitated complexes were eluted with 100 μl of 100 mM Glycine buffer (pH 2.2) for 10 minutes at RT and neutralized by adding 1/10 volume of 1M Tris-HCl pH 8.5.

The immunopurified protein complexes obtained from ZFP217 antibody were mixed in a ratio of 1:1 with digestion buffer (100 mM Tris-HCl, pH 8.5, 8M urea), reduced, alkylated and digested by sequential addition of lys-C and trypsin proteases as described (Kaiser and Wohlschlegel, 2005; Wohlschlegel, 2009). The digested peptide mixture was desalted and fractionated online using a 75 μM inner diameter fritted fused silica capillary column with a 5 μM pulled electrospray tip and packed in-house with 15 cm of Luna C18 3 μM reversed phase particles. The gradient was delivered by an easy-nLC 1000 ultra high-pressure liquid chromatography (UHPLC) system (Thermo Scientific). MS/MS spectra were collected on a Q-Exactive mass spectrometer (Thermo Scientific)(Kelstrup et al., 2012; Michalski et al., 2011). Data analysis was performed using the ProLuCID and DTASelect2 implemented in the Integrated Proteomics Pipeline - IP2 (Integrated Proteomics Applications, Inc., San Diego, CA) (Cociorva et al., 2007; Tabb et al., 2002). Protein and peptide identifications were filtered using DTASelect and considered at least two unique peptides per protein and a peptide-level false positive rate of less than 5% as estimated by a decoy database strategy (Elias and Gygi, 2007). Normalized spectral abundance factor (NSAF) values were calculated as described (Florens and Washburn, 2006).

Statistical Analysis

All values were expressed as mean ± SD. Statistical analysis was performed by the Unpaired Student's *t* test. A probability value of $p < 0.05$ was considered statistically significant.

SUPPLEMENTAL REFERENCES

(2012). An integrated encyclopedia of DNA elements in the human genome. Nature *489*, 57-74.
Ang, Y.S., Tsai, S.Y., Lee, D.F., Monk, J., Su, J., Ratnakumar, K., Ding, J., Ge, Y., Darr, H., Chang, B.*, et al.* (2011). Wdr5 mediates self-renewal and reprogramming via the embryonic stem cell core transcriptional network. Cell *145*, 183-197.
Arnold, C.D., Gerlach, D., Stelzer, C., Boryn, L.M., Rath, M., and Stark, A. (2013). Genome-wide quantitative enhancer activity maps identified by STARR-seq. Science *339*, 1074-1077.
Bailey, T.L., and Machanick, P. (2012). Inferring direct DNA binding from ChIP-seq. Nucleic Acids Res *40*, e128.
Brown, K.A., Pietenpol, J.A., and Moses, H.L. (2007). A tale of two proteins: differential roles and regulation of Smad2 and Smad3 in TGF-beta signaling. J Cell Biochem *101*, 9-33.
Clevers, H. (2006). Wnt/beta-catenin signaling in development and disease. Cell *127*, 469-480.
Cociorva, D., D, L.T., and Yates, J.R. (2007). Validation of tandem mass spectrometry database search results using DTASelect. Curr Protoc Bioinformatics *Chapter 13*, Unit 13 14.
Creyghton, M.P., Cheng, A.W., Welstead, G.G., Kooistra, T., Carey, B.W., Steine, E.J., Hanna, J., Lodato, M.A., Frampton, G.M., Sharp, P.A.*, et al.* (2010). Histone H3K27ac separates active from poised enhancers and predicts developmental state. Proc Natl Acad Sci U S A *107*, 21931-21936.
Dignam, J.D., Lebovitz, R.M., and Roeder, R.G. (1983). Accurate transcription initiation by RNA polymerase II in a soluble extract from isolated mammalian nuclei. Nucleic Acids Res *11*, 1475-1489.
Dominissini, D., Moshitch-Moshkovitz, S., Salmon-Divon, M., Amariglio, N., and Rechavi, G. (2013). Transcriptome-wide mapping of N(6)-methyladenosine by m(6)A-seq based on immunocapturing and massively parallel sequencing. Nat Protoc *8*, 176-189.
Elias, J.E., and Gygi, S.P. (2007). Target-decoy search strategy for increased confidence in large-scale protein identifications by mass spectrometry. Nat Methods *4*, 207-214.
Fidalgo, M., Faiola, F., Pereira, C.F., Ding, J., Saunders, A., Gingold, J., Schaniel, C., Lemischka, I.R., Silva, J.C., and Wang, J. (2012). Zfp281 mediates Nanog autorepression through recruitment of the NuRD complex and inhibits somatic cell reprogramming. Proc Natl Acad Sci U S A *109*, 16202-16207.
Fidalgo, M., Shekar, P.C., Ang, Y.S., Fujiwara, Y., Orkin, S.H., and Wang, J. (2011). Zfp281 functions as a transcriptional repressor for pluripotency of mouse embryonic stem cells. Stem Cells *29*, 1705-1716.
Florens, L., and Washburn, M.P. (2006). Proteomic analysis by multidimensional protein identification technology. Methods Mol Biol *328*, 159-175.
Hailesellasse Sene, K., Porter, C.J., Palidwor, G., Perez-Iratxeta, C., Muro, E.M., Campbell, P.A., Rudnicki, M.A., and Andrade-Navarro, M.A. (2007). Gene function in early mouse embryonic stem cell differentiation. BMC Genomics *8*, 85.
Heintzman, N.D., Hon, G.C., Hawkins, R.D., Kheradpour, P., Stark, A., Harp, L.F., Ye, Z., Lee, L.K., Stuart, R.K., Ching, C.W.*, et al.* (2009). Histone modifications at human enhancers reflect global cell-type-specific gene expression. Nature *459*, 108-112.
Heintzman, N.D., Stuart, R.K., Hon, G., Fu, Y., Ching, C.W., Hawkins, R.D., Barrera, L.O., Van Calcar, S., Qu, C., Ching, K.A.*, et al.* (2007). Distinct and predictive chromatin signatures of transcriptional promoters and enhancers in the human genome. Nat Genet *39*, 311-318.
Huang da, W., Sherman, B.T., and Lempicki, R.A. (2009a). Bioinformatics enrichment tools: paths toward the comprehensive functional analysis of large gene lists. Nucleic Acids Res *37*, 1-13.
Huang da, W., Sherman, B.T., and Lempicki, R.A. (2009b). Systematic and integrative analysis of large gene lists using DAVID bioinformatics resources. Nat Protoc *4*, 44-57.
Huang, G., Krig, S., Kowbel, D., Xu, H., Hyun, B., Volik, S., Feuerstein, B., Mills, G.B., Stokoe, D., Yaswen, P.*, et al.* (2005). ZNF217 suppresses cell death associated with chemotherapy and telomere dysfunction. Hum Mol Genet *14*, 3219-3225.

Jia, G., Fu, Y., Zhao, X., Dai, Q., Zheng, G., Yang, Y., Yi, C., Lindahl, T., Pan, T., Yang, Y.G., *et al.* (2011). N6-methyladenosine in nuclear RNA is a major substrate of the obesity-associated FTO. Nat Chem Biol *7*, 885-887.
Kagey, M.H., Newman, J.J., Bilodeau, S., Zhan, Y., Orlando, D.A., van Berkum, N.L., Ebmeier, C.C., Goossens, J., Rahl, P.B., Levine, S.S., *et al.* (2010). Mediator and cohesin connect gene expression and chromatin architecture. Nature *467*, 430-435.
Kaiser, P., and Wohlschlegel, J. (2005). Identification of ubiquitination sites and determination of ubiquitin-chain architectures by mass spectrometry. Methods Enzymol *399*, 266-277.
Kelstrup, C.D., Young, C., Lavallee, R., Nielsen, M.L., and Olsen, J.V. (2012). Optimized fast and sensitive acquisition methods for shotgun proteomics on a quadrupole orbitrap mass spectrometer. J Proteome Res *11*, 3487-3497.
Langmead, B., and Salzberg, S.L. (2012). Fast gapped-read alignment with Bowtie 2. Nat Methods *9*, 357-359.
Langmead, B., Trapnell, C., Pop, M., and Salzberg, S.L. (2009). Ultrafast and memory-efficient alignment of short DNA sequences to the human genome. Genome Biol *10*, R25.
Li, H., and Durbin, R. (2010). Fast and accurate long-read alignment with Burrows-Wheeler transform. Bioinformatics *26*, 589-595.
Lu, X., Goke, J., Sachs, F., Jacques, P.E., Liang, H., Feng, B., Bourque, G., Bubulya, P.A., and Ng, H.H. (2013). SON connects the splicing-regulatory network with pluripotency in human embryonic stem cells. Nat Cell Biol *15*, 1141-1152.
Machanick, P., and Bailey, T.L. (2011). MEME-ChIP: motif analysis of large DNA datasets. Bioinformatics *27*, 1696-1697.
Marson, A., Levine, S.S., Cole, M.F., Frampton, G.M., Brambrink, T., Johnstone, S., Guenther, M.G., Johnston, W.K., Wernig, M., Newman, J., *et al.* (2008). Connecting microRNA genes to the core transcriptional regulatory circuitry of embryonic stem cells. Cell *134*, 521-533.
McLean, C.Y., Bristor, D., Hiller, M., Clarke, S.L., Schaar, B.T., Lowe, C.B., Wenger, A.M., and Bejerano, G. (2010). GREAT improves functional interpretation of cis-regulatory regions. Nat Biotechnol *28*, 495-501.
Michalski, A., Damoc, E., Hauschild, J.P., Lange, O., Wieghaus, A., Makarov, A., Nagaraj, N., Cox, J., Mann, M., and Horning, S. (2011). Mass spectrometry-based proteomics using Q Exactive, a high-performance benchtop quadrupole Orbitrap mass spectrometer. Mol Cell Proteomics *10*, M111 011015.
Mikkelsen, T.S., Ku, M., Jaffe, D.B., Issac, B., Lieberman, E., Giannoukos, G., Alvarez, P., Brockman, W., Kim, T.K., Koche, R.P., *et al.* (2007). Genome-wide maps of chromatin state in pluripotent and lineage-committed cells. Nature *448*, 553-560.
Morey, L., Pascual, G., Cozzuto, L., Roma, G., Wutz, A., Benitah, S.A., and Di Croce, L. (2012). Nonoverlapping functions of the Polycomb group Cbx family of proteins in embryonic stem cells. Cell Stem Cell *10*, 47-62.
O'Loghlen, A., Munoz-Cabello, A.M., Gaspar-Maia, A., Wu, H.A., Banito, A., Kunowska, N., Racek, T., Pemberton, H.N., Beolchi, P., Lavial, F., *et al.* (2012). MicroRNA regulation of Cbx7 mediates a switch of Polycomb orthologs during ESC differentiation. Cell Stem Cell *10*, 33-46.
Ogawa, K., Saito, A., Matsui, H., Suzuki, H., Ohtsuka, S., Shimosato, D., Morishita, Y., Watabe, T., Niwa, H., and Miyazono, K. (2007). Activin-Nodal signaling is involved in propagation of mouse embryonic stem cells. J Cell Sci *120*, 55-65.
Qin, J., Whyte, W.A., Anderssen, E., Apostolou, E., Chen, H.H., Akbarian, S., Bronson, R.T., Hochedlinger, K., Ramaswamy, S., Young, R.A., *et al.* (2012). The polycomb group protein L3mbtl2 assembles an atypical PRC1-family complex that is essential in pluripotent stem cells and early development. Cell Stem Cell *11*, 319-332.
Rada-Iglesias, A., Bajpai, R., Swigut, T., Brugmann, S.A., Flynn, R.A., and Wysocka, J. (2011). A unique chromatin signature uncovers early developmental enhancers in humans. Nature *470*, 279-283.

Rahl, P.B., Lin, C.Y., Seila, A.C., Flynn, R.A., McCuine, S., Burge, C.B., Sharp, P.A., and Young, R.A. (2010). c-Myc regulates transcriptional pause release. Cell *141*, 432-445.
Salmon-Divon, M., Dvinge, H., Tammoja, K., and Bertone, P. (2010). PeakAnalyzer: genome-wide annotation of chromatin binding and modification loci. BMC Bioinformatics *11*, 415.
Spitzer, J., Hafner, M., Landthaler, M., Ascano, M., Farazi, T., Wardle, G., Nusbaum, J., Khorshid, M., Burger, L., Zavolan, M.*, et al.* (2014). PAR-CLIP (Photoactivatable Ribonucleoside-Enhanced Crosslinking and Immunoprecipitation): a step-by-step protocol to the transcriptome-wide identification of binding sites of RNA-binding proteins. Methods Enzymol *539*, 113-161.
Tabb, D.L., McDonald, W.H., and Yates, J.R., 3rd (2002). DTASelect and Contrast: tools for assembling and comparing protein identifications from shotgun proteomics. J Proteome Res *1*, 21-26.
Trapnell, C., Pachter, L., and Salzberg, S.L. (2009). TopHat: discovering splice junctions with RNA-Seq. Bioinformatics *25*, 1105-1111.
Trapnell, C., Williams, B.A., Pertea, G., Mortazavi, A., Kwan, G., van Baren, M.J., Salzberg, S.L., Wold, B.J., and Pachter, L. (2010). Transcript assembly and quantification by RNA-Seq reveals unannotated transcripts and isoform switching during cell differentiation. Nat Biotechnol *28*, 511-515.
Visel, A., Blow, M.J., Li, Z., Zhang, T., Akiyama, J.A., Holt, A., Plajzer-Frick, I., Shoukry, M., Wright, C., Chen, F.*, et al.* (2009). ChIP-seq accurately predicts tissue-specific activity of enhancers. Nature *457*, 854-858.
Wang, L., Feng, Z., Wang, X., and Zhang, X. (2010). DEGseq: an R package for identifying differentially expressed genes from RNA-seq data. Bioinformatics *26*, 136-138.
Wang, X., Lu, Z., Gomez, A., Hon, G.C., Yue, Y., Han, D., Fu, Y., Parisien, M., Dai, Q., Jia, G.*, et al.* (2014). N6-methyladenosine-dependent regulation of messenger RNA stability. Nature *505*, 117-120.
Wang, Z.X., Teh, C.H., Chan, C.M., Chu, C., Rossbach, M., Kunarso, G., Allapitchay, T.B., Wong, K.Y., and Stanton, L.W. (2008). The transcription factor Zfp281 controls embryonic stem cell pluripotency by direct activation and repression of target genes. Stem Cells *26*, 2791-2799.
Whyte, W.A., Bilodeau, S., Orlando, D.A., Hoke, H.A., Frampton, G.M., Foster, C.T., Cowley, S.M., and Young, R.A. (2012). Enhancer decommissioning by LSD1 during embryonic stem cell differentiation. Nature *482*, 221-225.
Wohlschlegel, J.A. (2009). Identification of SUMO-conjugated proteins and their SUMO attachment sites using proteomic mass spectrometry. Methods Mol Biol *497*, 33-49.
Yu, H.B., Johnson, R., Kunarso, G., and Stanton, L.W. (2011). Coassembly of REST and its cofactors at sites of gene repression in embryonic stem cells. Genome Res *21*, 1284-1293.
Yue, F., Cheng, Y., Breschi, A., Vierstra, J., Wu, W., Ryba, T., Sandstrom, R., Ma, Z., Davis, C., Pope, B.D.*, et al.* (2014). A comparative encyclopedia of DNA elements in the mouse genome. Nature *515*, 355-364.
Zhang, Y., Liu, T., Meyer, C.A., Eeckhoute, J., Johnson, D.S., Bernstein, B.E., Nusbaum, C., Myers, R.M., Brown, M., Li, W.*, et al.* (2008). Model-based analysis of ChIP-Seq (MACS). Genome Biol *9*, R137.